

# Performance of a large size triple GEM detector at high particle rate for the CBM Experiment at FAIR

Rama Prasad Adak<sup>a</sup>, Ajit Kumar<sup>b</sup>, A. K. Dubey<sup>b</sup>, Subhasis Samanta<sup>a</sup>, J. Saini<sup>b</sup>, S. Das<sup>a</sup>, S. Raha<sup>a</sup>, Subhasis Chattopadhyay<sup>b,a</sup>

<sup>a</sup>Centre for Astroparticle Physics & Space Science, Bose Institute, Block EN, Sector V, Salt Lake, Kolkata 700091, India and Department of Physics, Bose Institute, 93/1, A.P.C. Road, Kolkata 700009, India

<sup>b</sup>Variable Energy Cyclotron Centre, Sector-1, Block-AF, Salt Lake, Kolkata, India

arXiv:1604.02899v2 [physics.ins-det] 2 Jun 2016

## Abstract

In CBM Experiment at FAIR, dimuons will be detected by a Muon Chamber (MUCH) consisting of segmented absorbers of varying widths and tracking chambers sandwiched between the absorber-pairs. In this fixed target heavy-ion collision experiment, operating at highest interaction rate of 10 MHz for Au+Au collision, after the first MUCH detector station in its inner radial ring will face a particle rate of 1 MHz/cm<sup>2</sup>. To operate at such a high particle density, GEM technology based detectors have been selected for the first two stations of MUCH. We have reported earlier the performance of several small-size GEM detector prototypes built at VECC for use in MUCH. In this work, we report on a large GEM chamber prototype tested with proton beam of momentum 2.36 GeV/c at COSY-Jülich Germany. The detector was read out using nXYTER ASIC operated in self-triggering mode. An efficiency higher than 96% at  $\Delta V_{GEM} = 375.2$  V was achieved. The variation of efficiency with the rate of incoming protons has been found to vary within 2% when tested up to a maximum rate of 2.8 MHz/cm<sup>2</sup>. The gain was found to be stable at high particle rate with a maximum variation of ~ 9%.

*Keywords:*

Micro-pattern Gas Detector, CBM, Gas Electron Multiplier, Triple GEM detector, MUCH

## 1. Introduction

The Compressed Baryonic Matter experiment at FAIR [1] will explore the region of the phase diagram of strongly interacting matter at high baryon density and moderate temperature. This fixed target experiment will use proton to Au ions beams with maximum energy per nucleon,  $E_{lab}/A$  of 90 AGeV for protons and 35 AGeV for Au-ions colliding with various target nuclei. The experiment aims to study the chiral symmetry restoration, search for the phase transition, locate the critical end point, study the equation of state at high baryon density among other topics. The observables of this experiment include low mass vector mesons (LMVMs) like  $\rho, \omega$ , charmonia along with the collective flow of particles, their correlations and fluctuations. The main challenges include the measurement of low multiplicity, rare probes with high accuracy. In order to attain reasonable statistics for rare probes at a reasonable running period, the interaction rate of colliding ions in this experiment will reach ~ 10 MHz. In CBM, main tracking device is a set of silicon tracking stations (STS) placed inside a dipole magnet. The system measures the momentum of charged tracks with a resolution ( $\delta p/p$  of 1%). The LMVM like  $\rho, \omega, \phi$  and charmonia will be reconstructed from their decay into dileptons. The CBM Muon

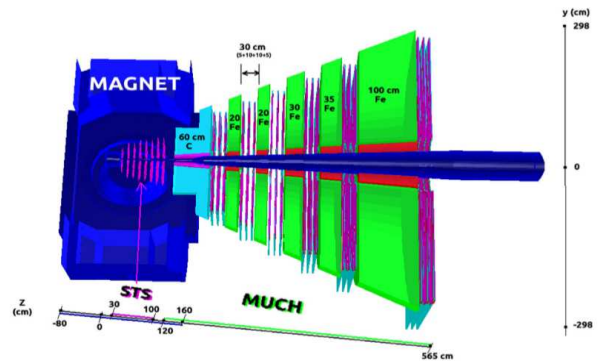


Figure 1: A schematic view of the MUCH of CBM Experiment with first absorber as carbon and rest are iron.

Chambers (MUCH) consists of alternating layers of hadron absorbers and detector stations to track muons. These segmented absorbers allow to identify muons over a wide range of momentum depending on the number of segments it passes. A schematic layout of MUCH is shown in Fig. 1. MUCH will cover an acceptance from  $\pm 5.6^\circ$  to  $\pm 25^\circ$ . The minimum value of the acceptance is the acceptance cover by the beam-pipe whereas the maximum value is the opening of the dipole magnet. MUCH will be operated in differ-

Email address: rpadak@jbose.ac.in (Rama Prasad Adak)

ent setup options by varying the positions of the absorber-detector combinations. The combinations include 3, 4, 5 or 6 such pairs for use in SIS100 and SIS300 energy regions of FAIR and two measurement options i.e., LMVM and charmonia. The first detector station of MUCH will have to face a hit density of  $0.1 / \text{cm}^2/\text{event}$  corresponding to  $1 \text{ MHz}/\text{cm}^2$  for interaction rate of  $10 \text{ MHz}$  of the colliding ions as obtained from GEANT3 simulations[2] using particles from UrQMD event generator[3] for central Au+Au collisions at  $E_{\text{lab}} = 25 \text{ AGeV}$ . The choice of the detector technology is guided by the rate capabilities of the detectors coupled to the cost to cover a large area. Considering the detector technologies presently available or under intense research and developing phase, Gas Electron Multiplier (GEM) [4] technology based chamber is found to be a suitable candidate. GEM based detectors has been used in CMS, COMPASS, PHENIX for their excellent rate handling capacity [5, 6, 7]. ALICE experiment will use triple-GEM detectors for their TPC upgrade to handle high rate of particles. CBM will use GEM chambers as their tracking detectors in the first two stations of the muon detection system. Towards this goal, we at VECC-India have built several triple GEM chambers of dimensions  $10 \text{ cm} \times 10 \text{ cm}$  and  $31 \text{ cm} \times 31 \text{ cm}$ . These chambers have been tested with X-rays [8], proton [9] and pion beams [10] to achieve  $> 95\%$  efficiency. Even after the successful development of these chambers, testing of two main criteria of their use in CBM-MUCH remain unfulfilled i.e., large size and high rate capability.

In this work, we report the development of a sector-shaped triple-GEM chamber of 80 cm length and 40 cm longer width. We also report the performance of the chamber using proton beams of momentum  $2.36 \text{ GeV}/c$  at the highest rate of  $2.8 \text{ MHz}/\text{cm}^2$ . The present chamber is considered as a prototype for the first station downstream of the magnet that faces the highest particle density. The 1<sup>st</sup> station of CBM will have 3 layers with 16 sector-shaped chambers in each layer.

The paper is organized as follows, in the next section, we discuss in somewhat details the layout of the GEM chambers for the CBM-MUCH. Section-3 contains the fabrication procedure of the GEM chamber including details of various components followed by the test setup, results and discussions in section 4 and 5 respectively.

## 2. Layout of chambers in CBM muon system

Fig. 2 shows the schematic diagram of a layer consisting of the sector-shaped chambers. Three such layers are to be mounted in a 30 cm gap between two successive absorbers. The number of sectors in each layer for the 1<sup>st</sup> and 2<sup>nd</sup> stations are 16 and 24 respectively. There will be a provision for a layer to be separated into two halves for servicing. For ease of production, all chambers in a particular station are identical. The sector-shaped chamber will be mounted back to back on two planes separated by an Aluminium plate. The active area of each sector will

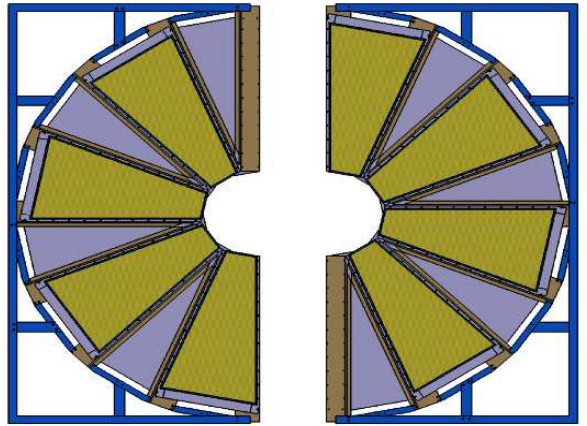


Figure 2: layout of sectors on a layer.

be somewhat larger than the area corresponding to  $360^\circ$  divided by the number of sectors. A single GEM chamber in the first station will cover  $23^\circ$  on azimuth including the overlap. This facilitates the overlap at the edges between two sectors. There are overlaps of  $0.5^\circ$  that corresponds to the mechanical support at the sides of the chambers.

## 3. Fabrication of the GEM chamber

Present chamber being discussed is a real size prototype chamber for the first station of MUCH. The design and the fabrication of readout PCB were carried out in India and the fabrication of other components and assembly were done at CERN.

### 3.1. GEM foils

This prototype triple GEM chamber is made of 3 standard single mask GEM foils. The drift gap, transfer gap and the induction gap of the chamber are  $3 \text{ mm}, 1 \text{ mm}, 1.5 \text{ mm}$  respectively. The GEM foils for the prototype chamber have been fabricated at the CERN. The GEM foils have the provision of stretching by NS-2 (no stretch, no spacer) technique[11]. The layout of the high voltage segmentation on the foil is shown in Fig. 3. The segmentation is made based on the occupancy of the chambers in Au+Au collisions at SIS-300 energy. Therefore, it is expected that the chamber will be able to handle particle rate at lower energy collisions available at SIS100 quite comfortably. Each GEM foil has been segmented into 24 sections on its upper surface. The innermost four sections were of  $25 \text{ cm}^2$ , rest are  $100 \text{ cm}^2$  area. Each of 24 sections was connected via a surface-mounted  $1 \text{ M}\Omega$  protection resistance. Four zones each having 6 segments were connected to independent power supplies using four resistive chains. For the  $100 \text{ cm}^2$  area with a  $1 \text{ M}\Omega$  protective resistance, calculation shows a voltage drop of  $0.4 \text{ V}$  due to a pulse current for a particle rate of  $10 \text{ MHz}$ . This drop in voltage does not change gain significantly.

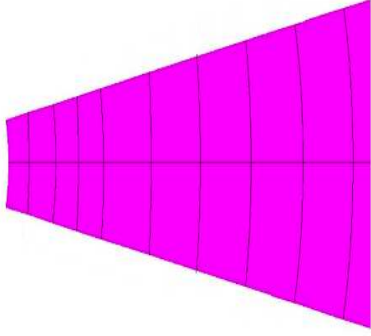


Figure 3: Layout of the HV segmentation on the GEM foil, only a part of the foil with only 20 segments have been shown.



Figure 4: Sector shaped readout PCB.

### 3.1.1. Drift Plane

The drift plane is a  $3\text{ mm}$  thick plane with copper clad on single side, fabricated at the CERN as per design from VECC. The drift printed circuit board (PCB) was extended laterally by  $5\text{ mm}$  in order to accommodate the HV lines for powering the segments. 14 holes each of  $2\text{ mm}$  diameter are made at appropriate positions to allow X-ray to pass through during testing. The holes are covered with mylar foils to make the chamber gas-tight.

### 3.2. Readout Plane

The anode readout PCB is an eight layered,  $2.7\text{ mm}$  thick PCB designed at VECC and fabricated in Bangalore, India. The PCB has  $1^\circ$  progressive size readout pads as shown in Fig. 4. The angle has been arrived at after simulations as mentioned in [12]. Each pad is a trapezium whose larger angles are  $90.5^\circ$ . This PCB has 23 pads in an annular ring and 79 pads in the radial direction. The

dimension of the readout pads are from  $3.9\text{ mm} \times 3.9\text{ mm}$  to maximum  $16.6\text{ mm} \times 16.6\text{ mm}$ . This way multi-hit probability on a pad is reduced. The coarse granularity of readout pads in the outermost region also drastically reduce the cost of the readout electronics. In total there are 1817 pads in the anode PCB.

#### 3.2.1. Assembly of the chamber

Some of the challenges that require special care for building the real size chamber are : (a) building of a large size chamber PCB (b) fabrication of a large size GEM foil (c) stretching of the large size foils and (d) proper layout of the tracks to accommodate the variation of occupancy. The job has been performed keeping in close contact with the RD51 team at CERN. We have used the NS-2 technique



Figure 5: GEM foil stretching using NS-2 technique, (top-left) special screws connected to spacers on the edge of the chamber, (top-right) A chamber ready for NS-2 stretching, (bottom-left) a GEM foil stretched and assembled, (bottom-right) view of several layers.

developed at CERN which has the advantages that (i) foils can be easily replaced (ii) no permanent gluing or thermal stretching is done and the foil could be reused, if required. The assembly of the chamber using NS-2 technique is shown in Fig. 5. First, brass pieces are fixed at the boundaries of the drift plane at a regular interval (Fig. 5.(top)). They act as support pillars with holes at prescribed intervals against which the foils will be stretched. A  $1\text{ mm}$  G10 spacer frame is placed between two foils to provide  $1\text{ mm}$  transfer gap. Thin metallic pins of appropriate size are soldered on the drift plane and passing through the spacers make contact with the respective GEM foils. Next



Figure 6: An assembled sector-shaped real-size chamber for the first station of the CBM muon chamber.

the readout plane is placed keeping  $1.5\text{ mm}$  induction gap. The entire chamber is sealed by the anode readout plane via an O ring. The screw pins are tightened to stretch the foils. Now the chamber is cleaned in an ultrasonic bath for some minutes. Finally, the chamber is made dry using an oven and put under  $Ar : CO_2$  gas. The Fig. 6 shows an assembled sector-shaped chamber showing the connecting points for the HV at the top attachment. All the design works were performed at VECC-Kolkata and the assembly of the large GEM chamber was performed at CERN.

#### 4. Test Beam Setup

A schematic layout of the experimental setup for testing the chamber is shown in Fig. 7. The GEM chamber was tested along with three Silicon Tracking Stations (STS) at the Jessica cave of COSY, Jülich, Germany using proton beam of momentum  $2.36\text{ GeV}/c$ . A pair of crossed optical fiber scintillators hodoscopes with the overlapping area of  $2\text{ cm} \times 2\text{ cm}$  placed at two ends of the setup has been used to form the beam trigger. The coincidence signals from the front and rear hodoscope scintillators were connected to the ReadOut Controller (ROC) for recording the timestamps of the beam particles. The detectors in this setup (STS, GEM, hodoscopes) were read out by using the nXYTER front end boards (FEB) directly connected to the chamber followed by the Readout controller (ROC). One ROC can handle two FEB boards. The readout PCB was divided into 15 regions, each one is read by one nXYTER that has 128 channels connected to 128 readout pads. nXYTER has one fast channel and another slow channel of peaking times  $30\text{ nanosecond}$  and  $140\text{ nanosecond}$  respectively and has a 12-bit ADC

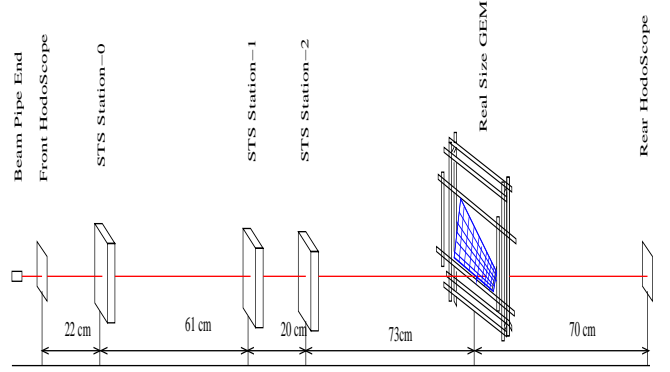


Figure 7: Experimental Setup at COSY, Jülich, Germany.

of  $25fC$  dynamic range. Data were collected in triggerless condition or in self-triggering mode. The nXYTER ASIC records the time-stamps of each hit on the detector above a predefined threshold. The time-stamps of all the hits above threshold are digitized and stored. Data were recorded for different beam intensities by adjusting the collimator windows. Data at different voltage-settings across the GEM foils were taken for different regions of the detector where readout pads of different sizes were exposed to the beam. All GEM foils in the chamber were kept at same voltage setting. A premixed gas mixture of argon (Ar) and carbon dioxide ( $CO_2$ ), mixed in 70:30 ratio by mass, was used.

#### 5. Results

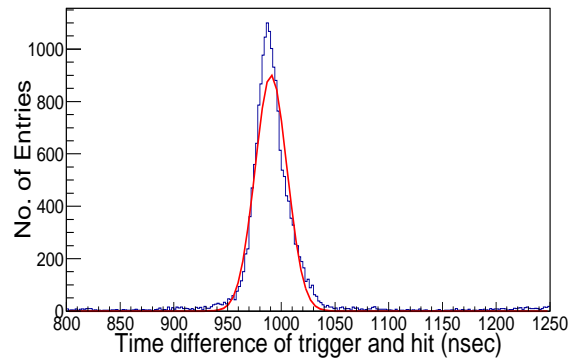


Figure 8: Distribution of the time difference between time-stamps of the trigger and GEM signals.

In a self-triggered readout system where all hits are stored along with their timestamps, first step of data analysis would be to find hits that are correlated in time with the trigger time stamps. A distribution of the difference in timestamps between coincidence trigger signal from the hodoscopes and those of the hits are shown in Fig. 8. The time correlation distribution is fitted with a Gaussian with

mean = 990.2 nanosecond and  $\sigma = 13.71$  nanosecond at a voltage across the GEM foil ( $\Delta V_{GEM}$ ) of = 371.8 V. The position of the peak depends on the cable delay in addition to the delay introduced by electronics. Almost no entries ( $\sim 3 - 4\%$ ) outside the peak region suggest that most of the hits are correlated with the trigger. The  $\sigma$  of the peak is a measure of the time resolution of the detector. The variation of  $\sigma$  with  $\Delta V_{GEM}$  at a fixed location is shown in Fig. 9. The variation has a minimum at 13.71 nanosecond at  $\Delta V_{GEM} = 371.8$  V. Hits lying inside the time correlation

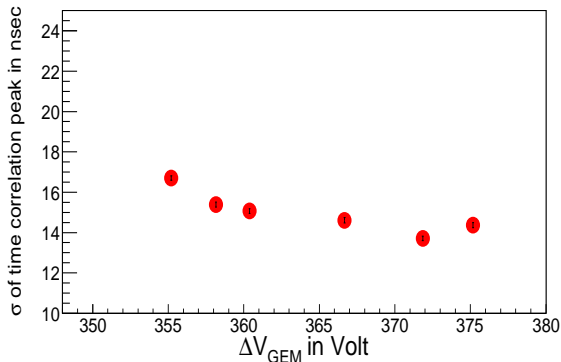


Figure 9: Variation of sigma of time correlation with  $\Delta V_{GEM}$ .

peak are related to beam particles and hence considered for further analysis. The positions of such hits on the GEM is shown in Fig. 10 for the region where the pad size was  $7.39 \text{ mm} \times 7.39 \text{ mm}$ . We get a narrow beam-spot for proton beam. The beam is mainly confined within a few pads.

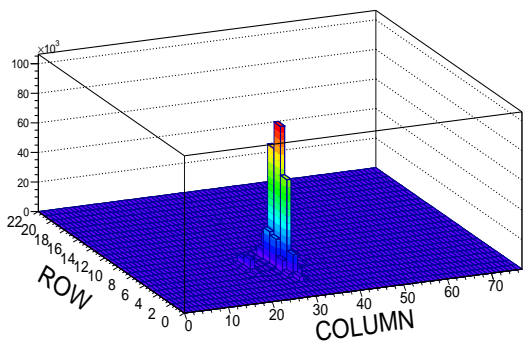


Figure 10: Proton beam spot on the GEM chamber in the region of pad size  $7.39 \text{ mm} \times 7.39 \text{ mm}$ .

In the next subsection, we will discuss different results on the chamber properties like ADC distribution, gain, efficiency among others in detail.

### 5.1. ADC distribution and chamber gain

ADC values of the hits within the time correlation window in an event are summed up to obtain the total ADC of a cluster in an event. The event-by-event

pedestal subtracted ADC distribution is shown in Fig. 11 for  $\Delta V_{GEM} = 366.7$  V. The distribution is fitted with a Landau distribution with MPV = 386.6. The MPV values

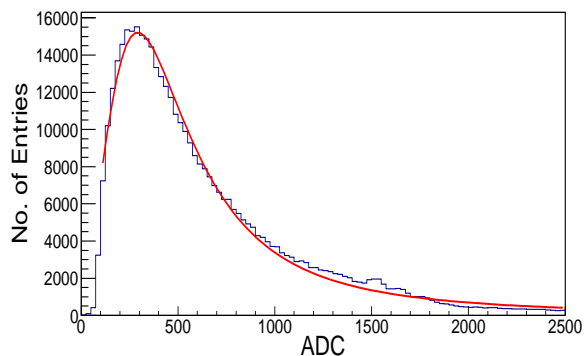


Figure 11: Pedestal subtracted cluster ADC distribution of the GEM chamber.

of ADC distributions are calculated for different  $\Delta V_{GEM}$  on the GEM foil. The ADC distribution saturates at higher  $\Delta V_{GEM}$  due to limited dynamic range of the nXYTER. The MPV values are used to calculate the total charge collected by the chamber. The input charge is the charge of electrons created by primary ionization in a  $3 \text{ mm}$  drift gap. The number of primary electrons is taken to be 30. The gain of the triple GEM prototype rises linearly with voltage across each GEM foil as seen in Fig. 12. Pad by pad variation of gain is shown in Fig. 13 for 39 pads of varying dimensions from  $4.44 \text{ mm} \times 4.44 \text{ mm}$  to  $5.61 \text{ mm} \times 5.61 \text{ mm}$ . It is observed that the gain is reasonably uniform over the entire detector plane with a standard deviation of 12%.

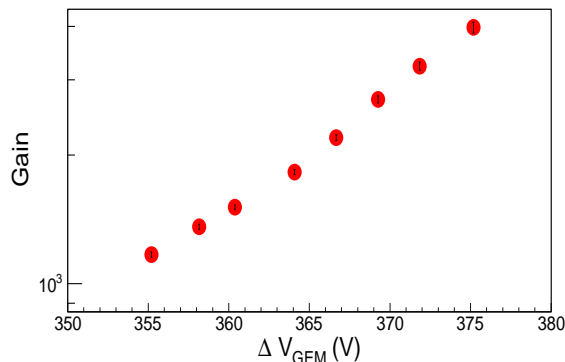


Figure 12: Variation of chamber gain with  $\Delta V_{GEM}$ .

We also estimate the stability of the gain because of increase of the rate of the incoming particles. The rate has been obtained by the difference between the average time intervals between two consecutive sets of 100 trigger signals. The gain is almost stable with a variation  $\sim 9\%$  at the highest rate of  $2.8 \text{ MHz/cm}^2$  as shown in Fig. 14.

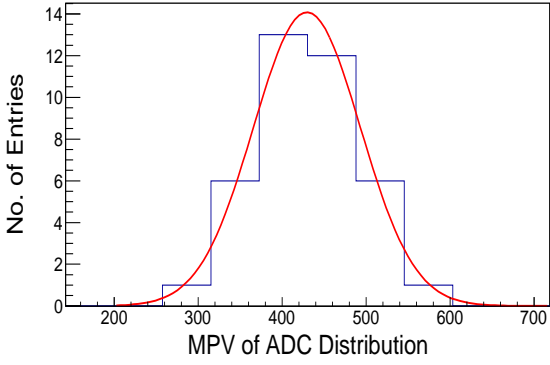


Figure 13: Uniformity of MPV of adc distribution for different channels with mean = 429.6 adc and sigma = 63.81 at  $\Delta V_{GEM} = 369.3 V$ .

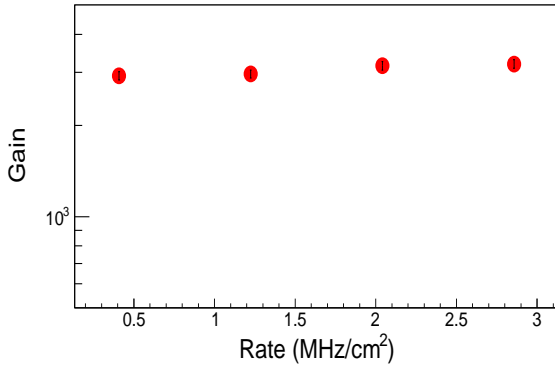


Figure 14: Stability of gain with the rate of beam particles.

### 5.2. Cell Multiplicity

Cell multiplicity is calculated using the hits within the selected time correlation window. The average cell multiplicity is slowly increasing with  $\Delta V_{GEM}$  from 1.2 at  $\Delta V_{GEM} = 355.2 V$  to 1.6 at  $\Delta V_{GEM} = 375.2 V$  as can be seen from Fig. 15. Due to the increase in voltage across GEM, the gain increases resulting in an increase of transverse size of the cluster profile.

### 5.3. Efficiency

The GEM detector will be used for tracking muons in CBM, so to operate the GEM detector in CBM-MUCH at high interaction rate the efficiency of the detector should be  $> 95\%$ . As the GEM detector is aligned with the hodoscopes, the particles that have correlated hits on both the front and rear hodoscopes are taken as the input particle on to the GEM. Particles are said to be detected if it has at least one hit on the GEM chamber within the time correlation window. The ratio of the number of detected particles as defined above and the number of triggers in a given time interval gives the efficiency of the detector. The variation of efficiency with  $\Delta V_{GEM}$  is shown for time windows of  $2\sigma$ ,  $3\sigma$ ,  $4\sigma$ ,  $5\sigma$  of the time correlation spectra. The study of the window size shows that a size of  $3\sigma$

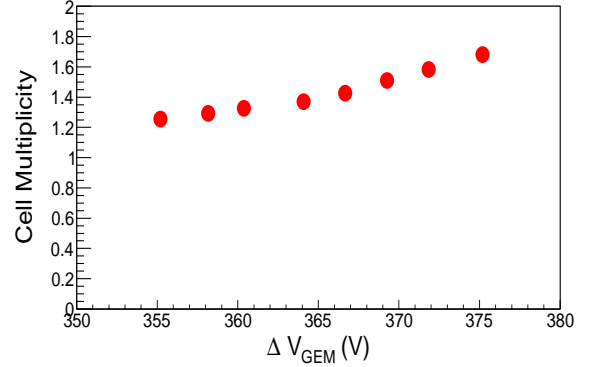


Figure 15: Variation of cell multiplicity with  $\Delta V_{GEM}$ , the size of the error bars are smaller than symbol size.

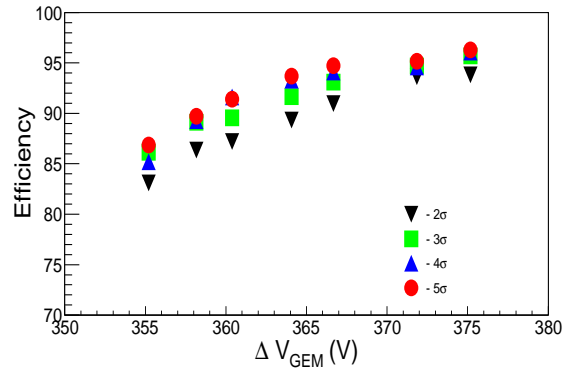


Figure 16: Efficiency with  $\Delta V_{GEM}$  for different time correlation distribution window, the size of the error bars are smaller than the symbol size.

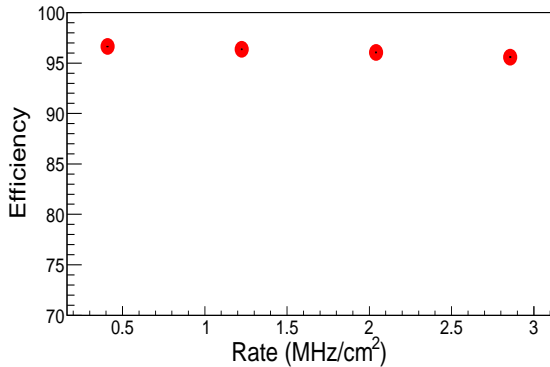


Figure 17: Variation of efficiency with rate of incoming particle.

seems optimum. The efficiency increases with  $\Delta V_{GEM}$  of the detector and reaches 96% at  $\Delta V_{GEM} = 375.2$  V for time windows equal to  $3\sigma$  as shown in Fig. 16. MUCH will be used in high interaction rate so efficiency should be stable for high rate of beam particles. The variation of efficiency with the average rate of the incoming particles is shown in Fig. 17. The efficiency at a fixed  $\Delta V_{GEM} = 375.2$  V is shown upto a beam rate of  $2.8$  MHz/cm<sup>2</sup>. The size of the beam is determined from its spot size on the hodoscopes. This rate is higher than the maximum particle-rate that the first MUCH detector has to face. As the particle rate increases efficiency decreases slightly ( $\sim 2\%$ ).

#### 5.4. Summary and discussions

The main challenge of MUCH detector is to handle high rate of incident particles. This is the first report on the performance of a real-size large GEM chamber suitable for the first MUCH chamber for its rate capability. A premixed Ar : CO<sub>2</sub> gas mixture in 70 : 30 ratio by mass is used. The detector was readout in self-triggered mode using the nXYTER. The hits on GEM detector are correlated in time to the signals produced by a pair of crossed scintillators hodoscopes one at the front and another at the rear position. The time correlation distribution is fitted by a Gaussian distribution with  $\sigma = 13.71$  nanosecond at  $\Delta V_{GEM} = 371.9$  V.  $\sigma$  is related to the time resolution of the detector. The efficiency of the detector reaches 96% at  $\Delta V_{GEM} = 375.2$  V. Cell multiplicity at this voltage for proton beam is 1.6. Cell multiplicity increases with  $\Delta V_{GEM}$  because the transverse size of the beam increases. The efficiency of the detector slightly decreases due to increase of the rate of the particle but the change is  $\sim 2\%$  (96.0% at  $0.4$  MHz/cm<sup>2</sup> to 94.8% at  $2.8$  MHz/cm<sup>2</sup> average particle-rate for  $\Delta V_{GEM} = 375.2$  V).

## 6. Acknowledgement

We thank S. K. Ghosh of Bose Institute, Kolkata, Walter Mueller, P. Senger of GSI-Darmstadt, L. Ropelski and E. Oliveri of RD51 for all help. We would also like to

thank the crew of COSY accelerator at Juelich, Germany. This work is supported by the DAE-SRC award under the scheme no. 2008/21/07 – BRNS/2738. The work has been funded by Department of Atomic Energy, Government of India and the Department of Science and Technology, Government of India. RP and SS thank two Indian funding agencies, University Grants Commission and Council of Scientific and Industrial Research for their grants with reference numbers F. No. 2 – 8/2002 (SA – I) and 09/015(0397)/2010 – EMR – I respectively.

## References

- [1] <https://www.gsi.de/work/forschung/cbmnqm/cbm.htm>.
- [2] R. Brun et al., GEANT3, CERN DD/EE/84-1, 1986.
- [3] S. Bass et al., Journal of Physics G: Nucl. Part. Phys., 25 (1999) 1859-1896.
- [4] F. Sauli, et al., Nucl. Instr. and Meth. A, 805 (2016) 2-24.
- [5] G. Bencivenni et al., Nucl. Instr. and Meth. A, 488 (2002) 493.
- [6] A. Bressan et al., Nucl. Instr. and Meth. A, 425 (1999) 262.
- [7] S. Bachmann et al., Nucl. Instr. and Meth. A, 470 (2001) 548-561.
- [8] A.K. Dubey et al., Nucl. Instr. and Meth. A, 718 (2013) 418-420.
- [9] CBM Progress Report 2013, GSI, Darmstadt
- [10] A.K. Dubey et al., Nucl. Instr. and Meth. A, 755 (2014) 62-68.
- [11] L. Franconi et al, Status of no-stretch no-spacer GEM assembly, the NS2 technique method and experiment result, 2012.
- [12] S. Ahmed et al., Nucl. Instr. and Meth. A, 775 (2015) 139-147.